

## Structural Fluctuations in the Spin-Liquid State of $\text{Tb}_2\text{Ti}_2\text{O}_7$

J. P. C. Ruff,<sup>1</sup> B. D. Gaulin,<sup>1,2</sup> J. P. Castellán,<sup>1</sup> K. C. Rule,<sup>1</sup> J. P. Clancy,<sup>1</sup> J. Rodriguez,<sup>1</sup> and H. A. Dabkowska<sup>1</sup>

<sup>1</sup>*Department of Physics and Astronomy, McMaster University, Hamilton, Ontario, L8S 4M1, Canada*

<sup>2</sup>*Canadian Institute for Advanced Research, 180 Dundas St. W., Toronto, Ontario, M5G 1Z8, Canada*

(Received 14 June 2007; published 5 December 2007; publisher error corrected 6 December 2007)

High-resolution x-ray scattering measurements on single crystal  $\text{Tb}_2\text{Ti}_2\text{O}_7$  reveal finite structural correlations at low temperatures. This geometrically frustrated pyrochlore is known to exhibit a spin-liquid or cooperative paramagnetic state at temperatures below  $\sim 20$  K. Parametric studies of structural Bragg peaks appropriate to the  $Fd\bar{3}m$  space group of  $\text{Tb}_2\text{Ti}_2\text{O}_7$  reveal substantial broadening and peak intensity reduction in the temperature regime 20 K to 300 mK. We also observe a small, anomalous lattice expansion on cooling below a density maximum at  $\sim 18$  K. These measurements are consistent with the development of fluctuations above a cooperative Jahn-Teller, cubic-tetragonal phase transition at very low temperatures.

DOI: [10.1103/PhysRevLett.99.237202](https://doi.org/10.1103/PhysRevLett.99.237202)

PACS numbers: 75.25.+z, 75.40.-s, 78.70.Ck

A magnetic material whose lattice geometry prevents the simultaneous satisfaction of the local magnetic interactions is said to be geometrically frustrated. Such materials, many of which are based on triangular and tetrahedral crystalline architectures, are of intense current interest because they have a natural proclivity towards exotic quantum mechanical ground states [1]. As the leading magnetic interactions on such lattices are frustrated, rather subtle subleading terms in the Hamiltonian, such as interactions beyond nearest-neighbors, weak disorder, and the order-by-disorder mechanism, tend to determine the ultimate ground state of the material.

The rare-earth-metal titanates, with formula  $\text{A}_2\text{Ti}_2\text{O}_7$ , are a well-studied family of frustrated magnetic insulators. The *A*-site is occupied by a trivalent rare-earth-metal ion with eightfold oxygen coordination, while the  $\text{Ti}^{4+}$  ion has sixfold oxygen coordination. Both the  $\text{A}^{3+}$  site and the  $\text{Ti}^{4+}$  site independently reside on the pyrochlore structure, a face-centered cubic lattice of corner-sharing tetrahedra which is a playground for phenomena related to geometrical frustration. Depending on the nature of the magnetic rare-earth-metal ion in these materials, their ground states can exhibit long-range magnetic order [2,3], spin ice physics [4,5], and in the case of  $\text{Tb}_2\text{Ti}_2\text{O}_7$ , a highly correlated quantum disordered state known as a collective paramagnet or spin liquid [6–8].

The low temperature properties of  $\text{Tb}_2\text{Ti}_2\text{O}_7$  have been extensively studied. However, the crystal lattice is generally assumed to be a passive bystander to the spin-liquid physics. In this Letter, we present high-resolution x-ray scattering evidence for strong fluctuations in the low temperature lattice of  $\text{Tb}_2\text{Ti}_2\text{O}_7$ , signifying both a feedback of frustration onto the crystal lattice and the importance of the lattice degrees of freedom in determining the exotic ground state of this material.

Current interest in  $\text{Tb}_2\text{Ti}_2\text{O}_7$  is largely due to its failure to attain magnetic order of any kind to temperatures as low

as 20 mK, despite having an antiferromagnetic (AFM) Curie-Weiss constant of  $\sim 18$  K [6–8]. Magnetic neutron scattering on  $\text{Tb}_2\text{Ti}_2\text{O}_7$  at low temperatures [8] shows diffuse scattering indicative of spin correlations over the spatial extent of a single tetrahedron ( $\sim 3.6$  Å) in zero magnetic field and ambient pressure. When perturbed with either relatively weak magnetic fields or applied pressures, or both, long-range magnetic order can be induced at temperatures of  $\sim 1$ – $3$  K [9–11].

Low lying crystal field levels for  $\text{Tb}^{3+}$  in this environment have been measured [12], and they are consistent with local [111] anisotropy, such that Tb moments are constrained to point into or out of the tetrahedra. However, the diffuse magnetic neutron scattering [7] as well as the presence of dispersive spin waves in the magnetic field-induced ordered state [9] of  $\text{Tb}_2\text{Ti}_2\text{O}_7$  at low temperatures are more easily understood in terms of continuous spin symmetries. This quandary has been recognized and discussed for some time [13,14].

Much earlier magneto-elastic measurements on  $\text{Tb}_2\text{Ti}_2\text{O}_7$  revealed both giant magnetostriction [15] and an anomalous Young's modulus [16] at low temperatures, indicating the importance of the coupling between magnetic and lattice degrees of freedom. Strong magneto-elastic effects have also been topical in cubic spinel antiferromagnets. The spinels have chemical composition  $\text{AB}_2\text{O}_4$ , and the *B*-sublattice ions also reside on a pyrochlore lattice. Strongly first order structural and magnetic phase transitions can occur simultaneously in some of these materials at low temperatures. In the case of  $\text{ZnCr}_2\text{O}_4$ , this occurs near 12.5 K, wherein the low temperature lattice undergoes a tetragonal distortion [17,18]. Other spinels exhibit unexpected plateaus in their magnetization as a function of field at low temperature which have been of intense interest [19,20]. These have been modeled using biquadratic exchange terms in the effective spin Hamiltonian of these materials, arising from strong

magneto-elastic coupling [21]. Theoretically, spin-Peierls-like distortions of the pyrochlore lattice which act to better satisfy frustrated AFM interactions have been predicted [22]. No such transition has been observed in  $\text{Tb}_2\text{Ti}_2\text{O}_7$  despite several systematic studies [23,24].

Large single crystals of  $\text{Tb}_2\text{Ti}_2\text{O}_7$  and  $\text{Y}_2\text{Ti}_2\text{O}_7$  were grown at McMaster University using the floating zone technique, and a two-mirror, NEC image furnace. Both crystals were grown at a rate of 6 mm/h in an Ar environment. The growth protocol was similar to that originally reported for  $\text{Tb}_2\text{Ti}_2\text{O}_7$  [25]. Samples with approximately cubic dimensions and  $1 \text{ mm}^3$  volumes were subsequently cut from the larger growths for use in the x-ray measurements. The samples were aligned with their  $(H, K, 0)$  plane coincident with the scattering plane, and placed in a Janis  $^3\text{He}$  cryostat mounted within a four-circle x-ray diffractometer. Cu  $K\alpha_1$  radiation from an 18 kW rotating anode x-ray generator was selected using a perfect single crystal germanium (110) monochromator. The diffracted beam was measured using a Bruker Histar area detector, mounted on the scattering arm at a distance of 0.7 m from the sample. This configuration allows for high-resolution characterization of Bragg peaks from room temperature down to  $\sim 300 \text{ mK}$ , with a temperature stability of  $\sim 10 \text{ mK}$ .

Measurements were carried out on both  $\text{Tb}_2\text{Ti}_2\text{O}_7$  and  $\text{Y}_2\text{Ti}_2\text{O}_7$  as a function of temperature for two high-angle Bragg reflections in the  $(H, K, 0)$  plane, the  $(12, 0, 0)$  and  $(8, 8, 0)$  Bragg peaks. Representative two-dimensional maps at  $T = 40 \text{ K}$  and  $T = 0.3 \text{ K}$  are shown in Fig. 1. The longitudinal and transverse (relative to the relevant reciprocal-lattice vector) directions in reciprocal space are indicated by the arrows and straight lines, respectively,

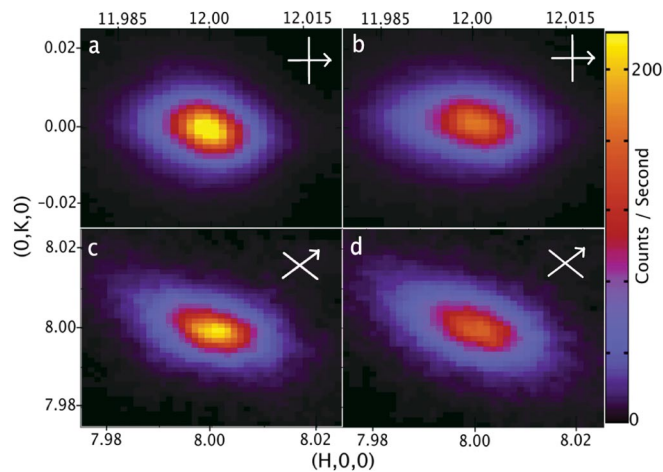


FIG. 1 (color).  $(H, K, 0)$  reciprocal space maps of structural Bragg peaks of  $\text{Tb}_2\text{Ti}_2\text{O}_7$ . (a)  $(12, 0, 0)$  at  $T = 40 \text{ K}$ . (b)  $(12, 0, 0)$  at  $T = 0.3 \text{ K}$ . (c)  $(8, 8, 0)$  at  $T = 40 \text{ K}$ . (d)  $(8, 8, 0)$  at  $T = 0.3 \text{ K}$ . Longitudinal (arrowhead) and transverse directions in reciprocal space are indicated in each panel. The low temperature broadening of the Bragg peaks is preferentially longitudinal for  $(12, 0, 0)$  and preferentially transverse for  $(8, 8, 0)$ .  $[H, K, L]$  are measured in reciprocal-lattice units (r.l.u.).

superposed on the figure. At low temperatures, the peak intensities of both reflections are suppressed, and the width of the scattering substantially increases as compared to the same data at  $40 \text{ K}$ . A careful inspection of the data shows that the  $(12, 0, 0)$  Bragg peak broadens preferentially in the longitudinal  $(H, 0, 0)$  direction, while the  $(8, 8, 0)$  reflection broadens preferentially in the transverse  $(H, -H, 0)$  direction. In each case, the integrated intensity of the peaks in Fig. 1 shows no temperature dependence.

Cuts through these maps at  $T = 20 \text{ K}$  and  $T = 0.3 \text{ K}$  are shown in Fig. 2, highlighting the dominant broadening for each peak. In both cases, it is clear that the peak widths increase substantially as the temperature is lowered into the spin-liquid regime appropriate to  $\text{Tb}_2\text{Ti}_2\text{O}_7$ . Similar high-resolution x-ray scattering measurements were carried out on the nonmagnetic pyrochlore  $\text{Y}_2\text{Ti}_2\text{O}_7$ , which shows no corresponding anomalous broadening or Bragg intensity variation. We conclude that  $\text{Tb}_2\text{Ti}_2\text{O}_7$  develops finite spatial lattice correlations below  $\sim 20 \text{ K}$ . We will argue that this is consistent with a system approaching a cooperative Jahn-Teller phase transition—albeit at unobtainably low temperatures.

The top panel of Fig. 3 shows the temperature dependence of the peak intensity at the  $(12, 0, 0)$  and  $(8, 8, 0)$  Bragg positions in  $\text{Tb}_2\text{Ti}_2\text{O}_7$ . The temperature dependence at the  $(12, 0, 0)$  Bragg position in  $\text{Y}_2\text{Ti}_2\text{O}_7$  is also shown for comparison. Both Bragg intensities in  $\text{Tb}_2\text{Ti}_2\text{O}_7$  decrease by about 20% between 20 and  $0.3 \text{ K}$ , and the decrease is continuous. No corresponding effect is seen in  $\text{Y}_2\text{Ti}_2\text{O}_7$ . The data shown in Figs. 1 and 2 was also fit to an Ornstein-Zernike form for spatial correlations [Eq. (1)] in order to extract inverse correlation lengths along both the longitudinal and transverse directions

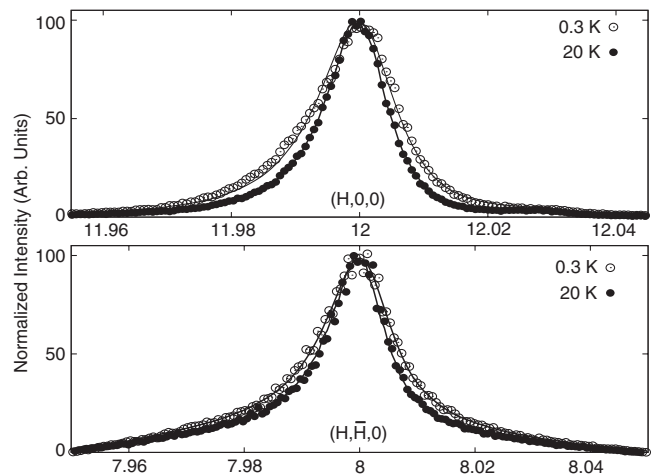


FIG. 2. Cuts through the  $\text{Tb}_2\text{Ti}_2\text{O}_7$  Bragg peaks, at both high and low temperatures, along with fits (solid lines) of the data to resolution convoluted Lorentzians, as described in the text. Intensities have been normalized to highlight the change in width. Top: Longitudinal broadening of the  $(12, 0, 0)$  peak. Bottom: Transverse broadening of the  $(8, 8, 0)$  peak.

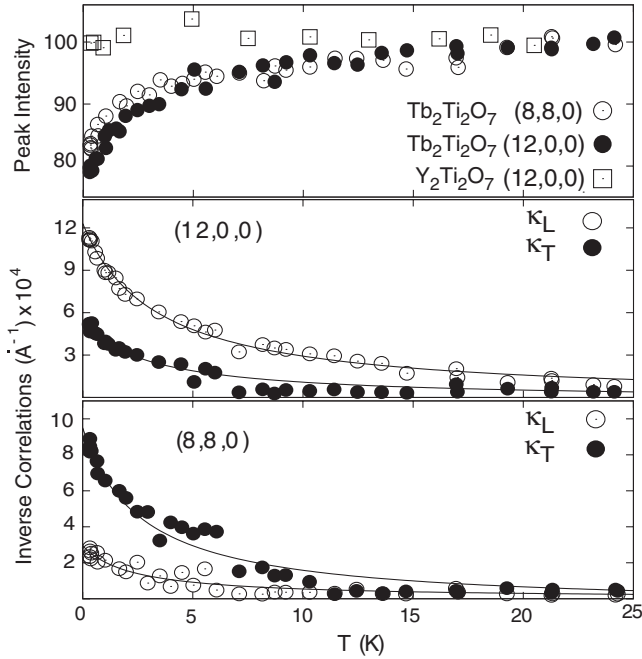


FIG. 3. Top: Temperature variation of peak intensities in  $\text{Tb}_2\text{Ti}_2\text{O}_7$  and  $\text{Y}_2\text{Ti}_2\text{O}_7$ . Middle: Inverse correlation lengths in both principal directions extracted from the  $(12, 0, 0)$  Bragg peak in  $\text{Tb}_2\text{Ti}_2\text{O}_7$ . Bottom: Similarly extracted correlation lengths from the  $(8, 8, 0)$  Bragg peak in  $\text{Tb}_2\text{Ti}_2\text{O}_7$ . The solid lines are guides to the eye.

$$S(q) = \frac{A}{1 + \left(\frac{q - q_0}{\kappa}\right)^2}. \quad (1)$$

Here,  $\kappa$  is the inverse correlation length in the appropriate direction. The data was fit using resolution convolution techniques wherein the  $T = 40$  K peak served as the resolution function. Inverse correlation lengths extracted from this analysis along the longitudinal (open symbols) and transverse (closed symbols) directions in reciprocal space are shown for the  $(12, 0, 0)$  and  $(8, 8, 0)$  Bragg peaks of  $\text{Tb}_2\text{Ti}_2\text{O}_7$  in the middle and bottom panels of Fig. 3, respectively.

Two features are clear from the measured inverse correlation lengths. First, the structure departs from long-range order at temperatures as high as 20 K, and spatial correlations diminish continuously as the temperature is lowered to  $\sim 0.3$  K. At the lowest temperatures, the spatial correlations still comprise many ( $\sim 80$ ) unit cells. Nevertheless, the increase in peak width indicating the reduction in correlation length is clear (see Fig. 2). Second, the broadening of the Bragg peaks is anisotropic. The longitudinal inverse correlation length at the  $(12, 0, 0)$  Bragg position and  $T = 0.3$  K is a factor of  $\sim 2.5$  greater than the transverse inverse correlation length. At the  $(8, 8, 0)$  Bragg position, the anisotropy is reversed at the lowest temperatures. A simple extrapolation of the data gives finite inverse correlation lengths at zero temperature.

The anisotropy in the inverse correlation lengths at both the  $(12, 0, 0)$  and  $(8, 8, 0)$  Bragg positions in  $\text{Tb}_2\text{Ti}_2\text{O}_7$  is qualitatively consistent with cubic-to-tetragonal structural fluctuations preceding a cooperative Jahn-Teller phase transition. A nonzero temperature cubic-to-tetragonal structural transition would introduce a second, distinct lattice parameter into the structure. This would result in the  $(12, 0, 0)$  reciprocal-lattice vector (with  $|\mathbf{Q}| = 12 \times \frac{2\pi}{a}$ ) and the  $(0, 0, 12)$  reciprocal-lattice vector (with  $|\mathbf{Q}| = 12 \times \frac{2\pi}{c}$ ) splitting in the longitudinal direction in reciprocal space. Reciprocal-lattice vectors of the form  $(8, 8, 0)$  would also show some splitting in the longitudinal direction, although it would be smaller than that at the  $(12, 0, 0)$  Bragg position by a factor of  $\sim 3$ . The principal splitting at the  $(8, 8, 0)$  Bragg position would be expected in the transverse direction.

$\text{TbVO}_4$  and  $\text{TbAsO}_4$  show related behavior near and below their tetragonal-to-orthorhombic cooperative Jahn-Teller phase transitions at 33.1 and 29.0 K, respectively [26,27]. Similar high-resolution x-ray scattering measurements performed with the same experimental set up on these two materials show an extreme form of this pattern of splitting of Bragg peaks below  $T_C$  [28]. These materials undergo the tetragonal-to-orthorhombic transition with twinning, such that the splitting of the  $(12, 0, 0)$  Bragg peak is exclusively longitudinal, while that of the  $(8, 8, 0)$  Bragg peak is exclusively transverse. In addition, in a critical temperature regime above  $T_C$ , Bragg peaks which ultimately split below  $T_C$  exhibit the same type of broadening [longitudinal for Bragg peaks of the form  $(H, 0, 0)$  and transverse for Bragg peaks of the form  $(H, H, 0)$ ]. This is indicative of structural fluctuations above the cooperative Jahn-Teller phase transition. The anisotropic nature of both the broadening (above  $T_C$ ) and splitting (below  $T_C$ ) of the Bragg peaks is more extreme for  $\text{TbVO}_4$  and  $\text{TbAsO}_4$  than for the case of the correlation lengths shown in Fig. 3 for  $\text{Tb}_2\text{Ti}_2\text{O}_7$ . This is because the high temperature phase in  $\text{TbVO}_4$  and  $\text{TbAsO}_4$  is tetragonal rather than cubic.

Our high-resolution x-ray measurements also allow an accurate determination of the lattice parameter in  $\text{Tb}_2\text{Ti}_2\text{O}_7$  as a function of temperature. This is shown in Fig. 4, along with the corresponding behavior of the lattice parameter in  $\text{Y}_2\text{Ti}_2\text{O}_7$ . From room temperature to  $\sim 18$  K, we observe the normal thermal contraction of the lattice in both  $\text{Tb}_2\text{Ti}_2\text{O}_7$  and  $\text{Y}_2\text{Ti}_2\text{O}_7$ . Interestingly, below  $\sim 18$  K, the  $\text{Tb}_2\text{Ti}_2\text{O}_7$  lattice undergoes anomalous expansion which it maintains to our base temperature of  $\sim 0.3$  K. The inset to Fig. 4 highlights the regime of thermal expansion with decreasing temperature at low temperatures. In contrast, the lattice parameter of nonmagnetic  $\text{Y}_2\text{Ti}_2\text{O}_7$  is independent of temperature below 20 K, as is typical for most materials. While the unusual expansion of the lattice parameter at low temperatures in  $\text{Tb}_2\text{Ti}_2\text{O}_7$  is small ( $\frac{\Delta a}{a} < 10^{-4}$ ), it is both measurable and consistent with earlier anomalous bulk lattice properties in the same low

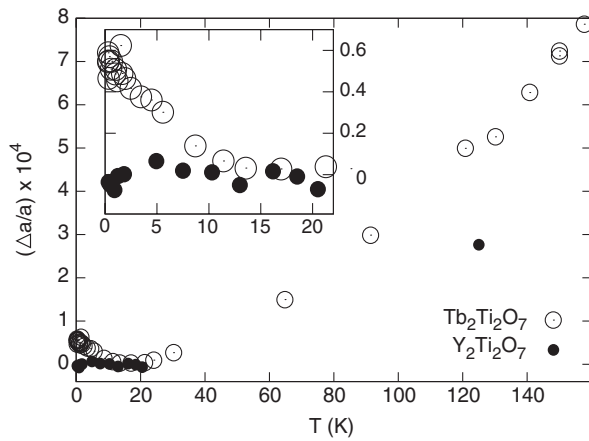


FIG. 4. Relative change in lattice constant as a function of temperature in both  $\text{Tb}_2\text{Ti}_2\text{O}_7$  and  $\text{Y}_2\text{Ti}_2\text{O}_7$ . Inset: Focus on the anomalous behavior within the spin-liquid regime of  $\text{Tb}_2\text{Ti}_2\text{O}_7$ .

temperature regime [15,16], and coincident with the appearance of the spin-liquid or cooperative paramagnetic state.

To conclude, high-resolution x-ray scattering measurements on  $\text{Tb}_2\text{Ti}_2\text{O}_7$  show continuous broadening below  $\sim 20$  K of allowed Bragg peaks, consistent with cubic-to-tetragonal fluctuations above a very low temperature cooperative Jahn-Teller phase transition. This fluctuation behavior of the lattice is coincident with the development of a highly correlated spin-liquid or cooperative paramagnetic ground state in  $\text{Tb}_2\text{Ti}_2\text{O}_7$ . The lowest temperature measurements therefore reveal a disordered ground state with coupled fluctuations in both the spin and lattice degrees of freedom.

We acknowledge useful conversations with G. M. Luke and M. J. P. Gingras. This work was supported by NSERC of Canada.

[1] See, for example: *Frustrated Spin Systems*, edited by H. T. Diep (World Scientific Publishing Co. Pte. Ltd., Singapore, 2004).

[2] J. D. M. Champion *et al.*, Phys. Rev. B **68**, 020401(R) (2003).

- [3] N. P. Raju, M. Dion, M. J. P. Gingras, T. E. Mason, and J. E. Greedan, Phys. Rev. B **59**, 14489 (1999).
- [4] M. J. Harris, S. T. Bramwell, D. F. McMorrow, T. Zeiske, and K. W. Godfrey, Phys. Rev. Lett. **79**, 2554 (1997).
- [5] B. C. den Hertog and M. J. P. Gingras, Phys. Rev. Lett. **84**, 3430 (2000).
- [6] J. S. Gardner *et al.*, Phys. Rev. Lett. **82**, 1012 (1999).
- [7] J. S. Gardner, B. D. Gaulin, A. J. Berlinsky, P. Waldron, S. R. Dunsiger, N. P. Raju, and J. E. Greedan, Phys. Rev. B **64**, 224416 (2001).
- [8] J. S. Gardner *et al.*, Phys. Rev. B **68**, 180401 (2003).
- [9] K. C. Rule *et al.*, Phys. Rev. Lett. **96**, 177201 (2006).
- [10] I. Mirebeau and I. N. Goncharenko, J. Phys. Condens. Matter **17**, S771 (2005).
- [11] I. Mirebeau, I. N. Goncharenko, G. Dhaleme, and A. Revcolevschi, Phys. Rev. Lett. **93**, 187204 (2004).
- [12] M. J. P. Gingras *et al.*, Phys. Rev. B **62**, 6496 (2000).
- [13] M. Enjalran and M. J. P. Gingras, Phys. Rev. B **70**, 174426 (2004).
- [14] H. R. Molavian, M. J. P. Gingras, and B. Canals, Phys. Rev. Lett. **98**, 157204 (2007).
- [15] I. V. Aleksandrov *et al.*, JETP **62**, 1287 (1985).
- [16] L. G. Mamsurova, K. S. Pigal'skii, and K. K. Pukhov, JETP Lett. **43**, 755 (1986).
- [17] S. H. Lee, C. Broholm, T. H. Kim, W. Ratcliff, II, and S. W. Cheong, Phys. Rev. Lett. **84**, 3718 (2000).
- [18] S.-H. Lee, C. Broholm, W. Ratcliff, G. Gasparovic, Q. Huang, T. H. Kim, and S.-W. Cheong, Nature (London) **418**, 856 (2002).
- [19] H. Ueda, H. A. Katori, H. Mitamura, T. Goto, and H. Takagi, Phys. Rev. Lett. **94**, 047202 (2005).
- [20] M. Matsuda *et al.*, Nature Phys. **3**, 397 (2007).
- [21] K. Penc, N. Shannon, Y. Motome, and H. Shiba, J. Phys. Condens. Matter **19**, 145267 (2007).
- [22] O. Tchernyshyov, R. Moessner, and S. L. Sondhi, Phys. Rev. B **66**, 064403 (2002).
- [23] O. Ofer, A. Keren, and C. Baines, J. Phys. Condens. Matter **19**, 145270 (2007).
- [24] S.-W. Han, J. S. Gardner, and C. H. Booth, Phys. Rev. B **69**, 024416 (2004).
- [25] J. S. Gardner, B. D. Gaulin, and D. McK Paul, J. Cryst. Growth **191**, 740 (1998).
- [26] G. A. Gehring and K. A. Gehring, Rep. Prog. Phys. **38**, 1 (1975).
- [27] Y. Hirano, N. Wakabayashi, C. K. Loong, and L. A. Boatner, Phys. Rev. B **67**, 014423 (2003).
- [28] M. J. Lewis, MSc. Thesis, McMaster University, 2002.